

Observation of two elastic thresholds in $\text{Ge}_x\text{As}_y\text{Se}_{1-x-y}$ glasses

R. P. Wang,^{1,a)} A. Smith,¹ B. Luther-Davies,¹ H. Kokkonen,² and I. Jackson²

¹Centre for Ultrahigh Bandwidth Devices for Optical Systems (CUDOS), Laser Physics Centre, Research School of Physics and Engineering, Australian National University, Canberra, ACT 0200, Australia

²Research School of Earth Sciences, Australian National University, Canberra, ACT 0200, Australia

(Received 20 October 2008; accepted 8 January 2009; published online 12 March 2009)

We have prepared $\text{Ge}_x\text{As}_y\text{Se}_{1-x-y}$ glasses with mean coordination numbers (MCNs) from 2.2 to 2.86. T_g was found to generally increase with increasing MCN while the glass density showed a maximum at $\text{MCN} \approx 2.45$ and a minimum at $\text{MCN} \approx 2.65$. The elastic moduli of the glasses were estimated from the shear and compressional wave velocities measured by ultrasonic pulse interferometry. For the first time we simultaneously observed two elastic transition thresholds, the first at $\text{MCN} \approx 2.45$ and the second at $\text{MCN} \approx 2.65$, which appear closely correlated with changes in the glass microstructure. The elastic moduli of two groups of samples with the same $\text{MCN} = 2.4$ and 2.64 but different compositions suggest that the chemical compositions also have an influence on the elastic properties. © 2009 American Institute of Physics. [DOI: 10.1063/1.3079806]

The purpose of measuring the elastic properties of $\text{Ge}_x\text{As}_y\text{Se}_{1-x-y}$ glasses is twofold. From a practical point of view, chalcogenide glasses are promising for both acousto-optic devices and acoustic delay lines due to their very high acousto-optic figure of merit, low acoustic attenuation, and low optical absorption in the near infrared region.^{1,2} However, there has been no systematic investigation of the acoustic properties of the Ge–As–Se glass system, and their dependence on the chemical composition of the glass is unknown. On the other hand, many physical properties of chalcogenide glasses have been found to correlate with the mean coordination number (MCN, defined as a sum of the respective elemental concentrations times their covalent coordination number), which is a measure of the network connectivity. By mean field theory using a counting constraint algorithm, Phillips and Thorpe³ first identified a floppy-to-rigid transition at $\text{MCN} = 2.4$. By considering self-organization of a random network, Boolchand and co-workers^{4–6} further found a rigid but stress-free intermediate phase (IP) from Raman scattering data and temperature-modulated differential scanning calorimetry. A thermally reversing compositional window was reported in the IP, where the glasses are generally nonaging. This behavior makes IP Ge–As–Se glasses very interesting for photonics applications since structural relaxation observed in most amorphous materials is detrimental to the stability of all photonic devices.⁷ The Boolchand IP in $\text{As}_x\text{Se}_{1-x}$ has been found to occur for MCN between 2.29 and 2.37, while in $\text{Ge}_x\text{As}_x\text{Se}_{1-2x}$ glasses containing the same concentrations of Ge and As it appears for MCN between 2.27 and 2.46.⁸ Recently, however, it was reported that the absence of aging within the so-called reversibility windows was not found in $\text{As}_x\text{Se}_{1-x}$ glasses that had been subjected to long-term physical aging.⁹ Therefore, further experiments for a wide compositional range are necessary to elucidate the correlation between the network structure, the physical properties, and MCN. Obviously, a starting

point to understand the IP is to examine the elastic response of the glassy network.

We, therefore, prepared 17 glasses with different compositions covering all the glass-forming regions including floppy, intermediate, and stressed rigid phases of the phase diagram.⁵ A detailed description about sample preparation can be found in our previous work.¹³ The glass transition temperature T_g was measured using a differential scanning calorimeter (DSC) (Shimadzu DSC-50) with 10 K/min scanning rate. The density ρ of the samples was measured using a Mettler H20 balance (Mettler-Toledo Ltd., Switzerland) with a MgO crystal used as a reference. Samples from each glass composition were weighed five times and the average density was recorded. Ultrasonic pulse interferometry was employed to measure both shear and compressional wave velocities at room temperature within the transducer response envelope centered at a resonant frequency of 20 MHz. The ultrasonic travel times were systematically corrected to reduce the effect of the bonding layer between the sample and the transducer.¹⁰ The shear C_s and compressional C_c elastic moduli were calculated using the formulas $C_s = \rho V_s^2$ and $C_c = \rho V_c^2$, where V_s and V_c are, respectively, the shear and compressional wave velocities. The errors in the measurements of both shear and compressional elastic moduli were estimated to be less than 0.5%.

Figure 1 shows the density of the $\text{Ge}_x\text{As}_y\text{Se}_{1-x-y}$ glasses as a function of MCN. For comparison, the data from Ref. 11 have also been included. The samples from two different sources exhibit similar behavior. For example, the density first increases with increasing MCN exhibiting a maximum at $\text{MCN} \approx 2.45$ before decreasing to a minimum at MCN around 2.65. For $\text{MCN} < 2.4$ corresponding, for example, to glass samples such as $\text{Ge}_5\text{As}_{10}\text{Se}_{85}$, $\text{Ge}_5\text{As}_{20}\text{Se}_{75}$, and $\text{Ge}_5\text{As}_{30}\text{Se}_{65}$, if there were no changes in the arrangement of the atoms in the glass, progressively replacing Se by As atoms should reduce the glass density because Se is heavier than As. Therefore, the observed opposite trend of increasing density with increasing MCN for $\text{MCN} < 2.4$ suggests that

^{a)}Electronic mail: rpw111@rpsphysse.anu.edu.au.

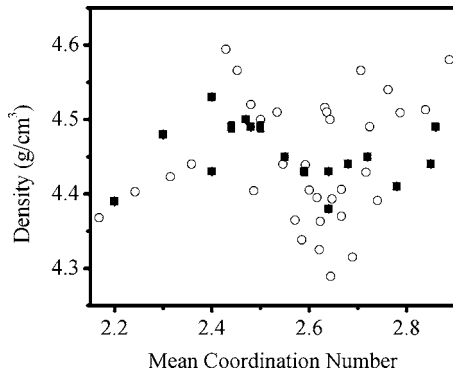


FIG. 1. Density of the $\text{Ge}_x\text{As}_y\text{Se}_{1-x-y}$ glasses from our results (solid squares and error bars) and from Ref. 11 (open circles).

the addition of As (or Ge) could result in significant changes to the topological structure of the glass.

Table I lists all the glass compositions and their corresponding MCN, V_s , V_c , C_s , and C_c . It is clear that T_g increases with increasing MCN except for the samples $\text{Ge}_5\text{As}_{38}\text{Se}_{57}$ and $\text{Ge}_{15}\text{As}_{34}\text{Se}_{51}$. These samples are located within or close to the nanoscale phase separation region of the phase diagram for the Ge–As–Se ternary glass. It is well established that T_g depends on the connectivity and thus on the rigidity of the vitreous network.^{12,13} Therefore increasing the concentration of Ge and As will result in a vitreous matrix with higher T_g . The appearance of phase separation can, however, destroy the backbone of the network and consequently cause a drop in T_g .^{4,5} Noteworthy is that in Table I, the glasses with same MCN of 2.4 exhibit almost the same T_g , emphasizing that T_g does depend on the network connectivity and hence MCN, rather than the particular chemical composition.

The acoustic velocities in Table I are in good agreement with the published values for samples with similar compositions. For example, Krause *et al.*² reported that V_s and V_c for

$\text{Ge}_{33}\text{As}_{12}\text{Se}_{55}$ glass were 1.432 and 2.518 km/s, respectively, about 4.5% higher than our results. Ohmachi and Uchida¹⁴ reported that V_s and V_c were 1.227 ± 0.002 and 2.250 ± 0.003 km/s, respectively, in As_2Se_3 , which are very close to the values we obtained for $\text{Ge}_5\text{As}_{30}\text{Se}_{65}$. Yun *et al.*¹⁵ reported that in $\text{Ge}_5\text{Se}_{95}$, V_s and V_c were 1.03 ± 0.02 and 1.88 ± 0.02 km/s, very close to our results for $\text{Ge}_5\text{As}_{10}\text{Se}_{85}$ where the values were 1.037 and 1.982 km/s, respectively.

The evolution of elastic moduli C_s and C_c as a function of MCN is plotted in Figs. 2(a) and 2(b). The key result is the simultaneous appearance of *two* transition thresholds at $\text{MCN} \approx 2.45$ and 2.65, respectively. Unlike the results reported in Refs. 16 and 17 where the elastic moduli below $\text{MCN} = 2.4$ were almost constant, we observed increasing moduli with increasing MCN for Se-rich samples such as $\text{Ge}_5\text{As}_{10}\text{Se}_{85}$, $\text{Ge}_5\text{As}_{20}\text{Se}_{75}$, and $\text{Ge}_5\text{As}_{30}\text{Se}_{65}$ glasses. The differences could be caused by the complete neglect of van der Waals interactions and dihedral angle forces in the theoretical treatment presented in Ref. 16, which are certainly needed to stabilize the structure in the floppy phase which exists for $\text{MCN} < 2.4$ and the inaccurate representation of MCN values in Ref. 17 due to the presence of 6%–8% oxygen impurity in their samples. Since the van der Waals interaction decreases with decreasing Se concentration in the three Se-rich samples, an increase in the elastic moduli becomes a natural result of introducing Ge and As.

For MCN between 2.45 and 2.65, C_s and C_c are almost constant at ≈ 68 and ≈ 230 kbar, respectively. Tanaka¹⁸ commented that this is due to a medium-range structural order. Between 2.4 and 2.65, several experimental results have confirmed that chalcogenide glasses have a layer-type structure which contain flexible segments.^{18–20} Thus, when compressing the samples, the van der Waals forces between the segments are mainly responsible for the moduli, while the covalent bonds within an individual segment are almost unperturbed by pressure. Therefore all the glasses have

TABLE I. A list of the prepared samples ordered by compositions, MCN, shear acoustic velocity V_s , compressional acoustic velocity V_c , shear elastic module C_s , and compressional module C_c .

| Composition | MCN | T_g (°C) | ρ (g/cm ³) | V_s (km/s) | V_c (km/s) | C_s (kbar) | C_c (kbar) |
|--|------|---------------|--------------------------------|-----------------|-----------------|-----------------|-----------------|
| $\text{Ge}_5\text{As}_{10}\text{Se}_{85}$ | 2.2 | 133.5 | 4.391 ± 0.002 | 1.037 | 1.982 | 47.19 | 172.49 |
| $\text{Ge}_5\text{As}_{20}\text{Se}_{75}$ | 2.3 | 145.2 | 4.475 ± 0.003 | 1.117 | 2.098 | 55.88 | 197.15 |
| $\text{Ge}_5\text{As}_{30}\text{Se}_{65}$ | 2.4 | 179.5 | 4.538 ± 0.001 | 1.222 | 2.248 | 67.62 | 229.00 |
| $\text{Ge}_{15}\text{As}_{10}\text{Se}_{75}$ | 2.4 | 179.3 | 4.427 ± 0.001 | 1.172 | 2.158 | 60.87 | 206.23 |
| $\text{Ge}_{11}\text{As}_{22}\text{Se}_{67}$ | 2.44 | 210.5 | 4.488 ± 0.006 | 1.240 | 2.240 | 69.08 | 225.29 |
| $\text{Ge}_{11.5}\text{As}_{24}\text{Se}_{64.5}$ | 2.47 | 236.7 | 4.495 ± 0.001 | 1.250 | 2.212 | 70.16 | 219.66 |
| $\text{Ge}_5\text{As}_{38}\text{Se}_{57}$ | 2.48 | 204.9 | 4.498 ± 0.001 | 1.193 | 2.212 | 64.10 | 220.15 |
| $\text{Ge}_{12.5}\text{As}_{25}\text{Se}_{62.5}$ | 2.5 | 247.9 | 4.493 ± 0.006 | 1.249 | 2.276 | 70.02 | 232.61 |
| $\text{Ge}_{15}\text{As}_{25}\text{Se}_{60}$ | 2.55 | 280.4 | 4.448 ± 0.001 | 1.242 | 2.261 | 68.65 | 227.46 |
| $\text{Ge}_{18}\text{As}_{23}\text{Se}_{59}$ | 2.59 | 293.4 | 4.434 ± 0.005 | 1.244 | 2.290 | 68.53 | 232.41 |
| $\text{Ge}_{22}\text{As}_{20}\text{Se}_{58}$ | 2.64 | 323.7 | 4.435 ± 0.001 | 1.254 | 2.284 | 69.68 | 231.02 |
| $\text{Ge}_{15}\text{As}_{34}\text{Se}_{51}$ | 2.64 | 285.9 | 4.384 ± 0.002 | 1.212 | 2.223 | 65.10 | 218.90 |
| $\text{Ge}_{22}\text{As}_{24}\text{Se}_{54}$ | 2.68 | 335.9 | 4.449 ± 0.002 | 1.274 | 2.306 | 72.01 | 236.12 |
| $\text{Ge}_{24}\text{As}_{24}\text{Se}_{52}$ | 2.72 | 353.1 | 4.437 ± 0.002 | 1.309 | 2.361 | 76.26 | 248.09 |
| $\text{Ge}_{33}\text{As}_{12}\text{Se}_{55}$ | 2.78 | 383.3 | 4.431 ± 0.001 | 1.369 | 2.435 | 82.43 | 260.85 |
| $\text{Ge}_{35}\text{As}_{15}\text{Se}_{50}$ | 2.85 | 404.3 | 4.441 ± 0.001 | 1.457 | 2.552 | 94.22 | 289.17 |
| $\text{Ge}_{33}\text{As}_{20}\text{Se}_{47}$ | 2.86 | 405.2 | 4.452 ± 0.001 | 1.506 | 2.648 | 100.9 | 311.2 |

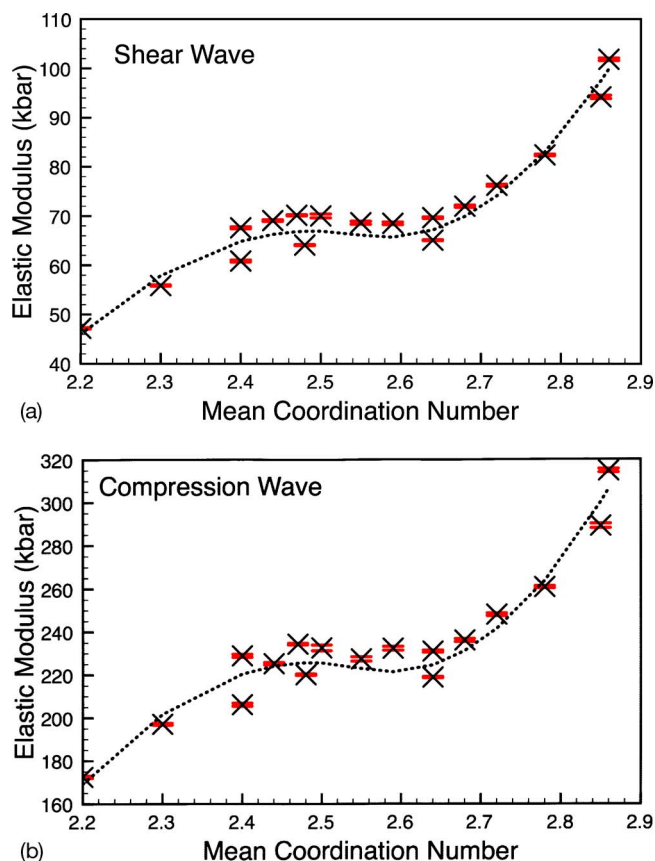


FIG. 2. (Color online) (a) The shear and (b) compressional elastic moduli and their error bars as a function of MCN. The solid lines correspond to least-squares fitting results.

moduli of similar magnitude, irrespective of their detailed microscopic structure.

For MCN values above 2.65, the segments will be cross linked by increasing Ge and As concentrations forming a stressed-rigid phase. A line fit to the data above MCN = 2.65 in Fig. 2(b) when projected to MCN=4 gives $C_c = 788.5$ kbar, which is comparable with crystalline Ge at 880 kbar where no van der Waals interaction exists. Tanaka reported that the constraint-counting formalism yields a value of MCN ~ 2.67 for transition to a rigid state if a two-dimensional layer structure is embedded in a 3-dimensional space.²¹ The transition we observed at 2.65 is, therefore, very close to that threshold.¹⁸

All previous attempts to search for elastic transitions in chalcogenide glasses failed to identify the existence of two transition thresholds. We cannot be absolutely certain as to whether these two transitions are specifically related to the IP that has been identified from Raman scattering and temperature-modulated DSC.^{4,5} We note that the elastic moduli of the samples located in nanophase separated regions of the phase diagram, including $\text{Ge}_5\text{As}_{38}\text{Se}_{57}$ and $\text{Ge}_{15}\text{As}_{34}\text{Se}_{51}$, do not deviate significantly from the general evolution of the elastic properties with MCN revealed in Fig. 2. Therefore, nanophase separation appears to have little effect on the elastic properties of the glasses. On the other hand, the elastic modulus at a particular MCN appears to be somewhat affected by chemical composition, for example, different values were obtained at MCN=2.4 for $\text{Ge}_5\text{As}_{30}\text{Se}_{65}$

and $\text{Ge}_{15}\text{As}_{10}\text{Se}_{75}$. In fact recently x-ray absorption fine structure spectroscopy indicated that chemical composition is a critical factor in determining the onset of the structural and topological transitions.²² Hence the changes in elastic moduli for the same MCN suggest that the chemical composition can have an influence on the elastic properties. Nevertheless, our results clearly demonstrate the existence of two transitions in elastic properties. The first at MCN around 2.45 is in agreement with previous results,^{3,16,17} while the second transition at 2.65 indicates that the most rigid Ge-Ge bonds are formed in strongly Se-deficient glass, as confirmed by our recent Raman scattering data.²³ This second threshold correlates with transition to a stressed-rigid phase identified by Tanaka.²¹

In summary, we prepared $\text{Ge}_x\text{As}_y\text{Se}_{1-x-y}$ glasses spanning a MCN from 2.2 and 2.86. T_g was found to increase with increasing MCN, except those glasses located within the nanoscale phase-separated regions of the phase diagram. The density of the glasses shows a maximum at 2.45 and a minimum at 2.65. The elastic moduli of the glasses were estimated from the shear and compressional wave velocities measured by the ultrasonic pulse interferometry. At the first time we simultaneously observed two elastic transition thresholds at MCN 2.45 and 2.65, which correlate with the structural transitions predicted for this ternary glass system.

This research is supported by the Australian Research Council through its Centres of Excellence and Federation Fellow Programs.

¹I. C. M. Littler, L. B. Fu, E. C. Magi, D. Pudo, and B. J. Eggleton, *Opt. Express* **14**, 8088 (2006).

²J. T. Krause, C. R. Kurkjian, D. A. Pinnow, and E. A. Sigety, *Appl. Phys. Lett.* **17**, 367 (1970).

³J. C. Phillips, *J. Non-Cryst. Solids* **34**, 153 (1979); M. F. Thorpe, *ibid.* **57**, 355 (1983).

⁴Y. Wang, P. Boolchand, and M. Micoulaut, *Europhys. Lett.* **52**, 633 (2000).

⁵T. Qu, D. G. Georgiev, P. Boolchand, and M. Micoulaut, *Mater. Res. Soc. Symp. Proc.* **754**, CC8.1.1 (2003).

⁶P. Boolchand, G. Lucovsky, J. C. Phillips, and M. F. Thorpe, *Philos. Mag.* **85**, 3823 (2005).

⁷R. P. Wang, A. V. Rode, S. J. Madden, C. J. Zha, R. A. Javis, and B. Luther-Davies, *J. Non-Cryst. Solids* **353**, 950 (2007).

⁸S. Chakravarty, D. G. Georgiev, P. Boolchand, and M. Micoulaut, *J. Phys.: Condens. Matter* **17**, L1 (2005).

⁹R. Golovchak, H. Jain, O. Shpotyuk, A. Kozdras, A. Saiter, and J. M. Saiter, *Phys. Rev. B* **78**, 014202 (2008).

¹⁰H. Niesler and I. Jackson, *J. Acoust. Soc. Am.* **86**, 1573 (1989).

¹¹Z. U. Borisova, *Glassy Semiconductors* (Plenum, New York, 1981).

¹²M. A. Popescu, *Non-Crystalline Chalcogenides* (Kluwer, Dordrecht, 2001).

¹³R. P. Wang, C. J. Zha, A. V. Rode, S. J. Madden, and B. Luther-Davies, *J. Mater. Sci.: Mater. Electron.* **18**, 419 (2007).

¹⁴Y. Ohmachi and N. Uchida, *J. Appl. Phys.* **43**, 1709 (1972).

¹⁵S. S. Yun, H. Li, R. L. Cappelletti, R. N. Enzweiler, and P. Boolchand, *Phys. Rev. B* **39**, 8702 (1989).

¹⁶H. He and M. F. Thorpe, *Phys. Rev. Lett.* **54**, 2107 (1985).

¹⁷B. L. Halfpap and S. M. Lindsay, *Phys. Rev. Lett.* **57**, 847 (1986).

¹⁸K. Tanaka, *Solid State Commun.* **60**, 295 (1986).

¹⁹C. Lin, L. E. Busse, and S. R. Nagel, *Phys. Rev. B* **29**, 5060 (1984).

²⁰K. Tanaka, *Solid State Commun.* **58**, 469 (1986).

²¹K. Tanaka, *Phys. Rev. B* **39**, 1270 (1989).

²²S. Sen, C. W. Ponader, and B. G. Aitken, *Phys. Rev. B* **64**, 104202 (2001).

²³R. P. Wang, A. Smith, A. Prasad, D. Y. Choi, and B. Luther-Davies, "Raman spectra of $\text{Ge}_x\text{As}_y\text{Se}_{1-x-y}$ glasses," *Phys. Rev. B* (submitted).